Simulation and investigations on the vibro-acoustic behavior of cylindrical shells in ice-covered water

Xianzhong Wang[a,b,c,□], Di Chen[c], Yeping Xiong[b], Weiguo Wu[a,c]

[a] Key Laboratory of High Performance Ship Technology (Wuhan University of Technology), Ministry of Education, Wuhan 430063, PR China

[b] Faculty of Engineering and the Environment, University of Southampton, Southampton, SO17 1BJ, United Kingdom

[c] School of Transportation, Wuhan University of Technology, Wuhan 430063, PR China

Abstract

Vibro-acoustic responses of cylindrical shells immersed in ice-covered water are typical acoustic-structure coupling problems. The dynamic model of the immersed cylindrical shell was established by Finite Element Method (FEM) to obtain the vibration response. The elastic constitutive material was adopted to simulate the ice model. The acoustic model of cylindrical shells was constructed by Boundary Element Method (BEM) to gain the underwater acoustic radiation. A series of boundary conditions were defined to tackle dynamic accurate contact interactions of the cylindrical shell, fluid field and ice model. Comparative analysis with the vibro-acoustic results of numerical model was proceeded to show the practicality and effectiveness of the numerical method. Both models of fully immersed and partially immersed cylindrical shells were calculated to analyze the vibration and underwater acoustic radiation. The effect of immersion depth, ice thickness, temperature and brine volume on vibro-acoustic responses of the immersed cylindrical shells were also discussed. It provides a way to evaluate the vibro-acoustic performance of underwater vehicles in polar ice area.

Key words: cylindrical shell; ice; vibration; acoustic radiation; experiment

1 Introduction

Most of the Arctic is covered by sea ice, which greatly limits the navigation of ships. The Arctic sea ice average thickness can reach 2m~4m[1-3]. The physical properties of ice provide special a more complex acoustic condition for the submarine's activities. And the excessive radiated noise from submarines in the ice-covered sea may also make a strong impact on marine animals. During the design and operation process of

* Corresponding author at: School of Transportation, Wuhan University of Technology, Wuhan 430063, China.
  E-mail address: xianzhongwang00@163.com (X. Wang)

the marine structures, accurate predictions of vibration and acoustic radiation of cylindrical shells in ice-covered oceans were becoming more and more important for satisfying the requirements of the increasing activities in Arctic regions [4].

Based on discrete element meshes and low order shape functions constructed, the vibro-acoustic response of immersed cylindrical shells can be obtained by numerical methods such as FEM [5], BEM [6] and coupled FEM and BEM [7]. Ettouney et al. [8] presented a finite difference method to solve the vibration and sound radiation of a submerged cylindrical shell with two hemispherical end closures and an interior beam. Peters et al. [9] investigated the influence of mass distribution and isolation on the acoustic characteristic of a submerged hull by a fully coupled BEM and FEM. Analytical methods are more suitable for the dynamic analysis of several typical elastic structures including cylindrical shells [10]. The wave propagation method was employed by Caresta and Kessissoglou [11-12] to solve the free vibration, forced vibration and sound radiation of submerged ring-stiffened cylindrical shells under axial excitation. A sub-structuring approach called the Condensed Transfer Function (CTF) method was proposed by Meyer et al. [13] to investigate the vibro-acoustic behaviour of a submerged cylindrical shell with non-axisymmetric internal structures. Wang et al. [14-15] presented a precise transfer matrix method (PTMM), solved a set of first-order differential equations and performed the vibro-acoustic analysis of submerged stiffened cylindrical shells and combined shells. After considering the effects of the ring-stiffeners constructed by discrete element stiffener theory, Qu et al. [16] derived a modified variational method and analyzed the free and forced vibration of ring-stiffened cylindrical shells under different boundary conditions. Guo et al. [17] presented an analytical method to solve the vibration response, employed the boundary element method to obtain the sound radiation and studied the far-field sound field distribution of a finite cylindrical shell submerged at finite depth from the water surface. At present, there is no public literature to aim at the vibration and acoustic radiation of cylindrical shells in ice-covered water.

Reliable numerical simulation of the ice model is one of the keys to study the acoustic property of ice-

covered sea. Many scholars have proposed different constitutive models for ice materials. At large and medium scales, Pritchard [18] investigated the stress and strain of sea ice and established its elastic-plastic constitutive model. Hibler [19] considered the rheological properties of sea ice, which is caused by fracture, overlap and accumulation at the same scales. A viscoplastic constitutive model of sea ice was established, but ignore the effects of the elastic deformation. Based on the experimental phenomena of ice model and ship models, Gagnon [20] proposed a foam model to simulate the ice material constitutive model which can effectively explain the melting phenomenon of ice in the collision zone. The interaction between ice model and two compliant rectangular structures with different structural properties was numerically simulated to analyze ice-induced vibrations and ice buckling [21]. Mattsson et al. [22] proposed a finite difference method to simulate acoustic and flexural gravity waves incompressible, inviscid fluids partially covered by a thin elastic layer. Scholars have paid more attention to the ice-breaking performance of polar navigation ships, and have established reliable experimental and numerical research methods. However, the research about underwater acoustic characteristics of submarines in the polar region is very rare. There is very few publicly available information related to the study on sound radiation of structures in an ice environment.

In this paper, the vibro-acoustic response of cylindrical shells in an ice environment is solved by coupled FEM and BEM. Based on Finite Element Method, both the cylindrical shell and ice model in the dynamic analysis are modelled by tetrahedron elements and hexahedron elements respectively to obtain the vibration response. The fluid domains are defined by infinite boundary condition and surface impedance boundary condition. A small contact between the ice model and the partially immersed cylindrical shell is developed, which means there are only small deformation assumption and no plastic deformation and failure of ice. The acoustic model of cylindrical shells was established by BEM to calculate the underwater acoustic radiation. The experiment model was designed to measure the vibro-acoustic responses and demonstrate the effectiveness and practicality of the present method by comparing with numerical results. Both dynamic models of fully and partially immersed cylindrical shells were calculated to analyze the underwater vibration

and acoustic radiation behaviours. The influence of submergence depth, brine volume, temperature and ice thickness on mean quadratic velocity level L_v, sound pressure level L_p, sound power level L_w, radiation efficiency level and the sound directivity of the cylindrical shell were also discussed.

2 Numerical formulations

2.1 Acoustic model

Fluid load p in the fluid medium should satisfy Helmholtz equation in the cylindrical coordinates, which can be written as

$$\frac{\partial^2 p}{\partial^2 r} + \frac{1}{r}\frac{\partial p}{\partial r} + \frac{1}{r^2}\frac{\partial^2 p}{\partial^2 \theta} + \frac{\partial^2 p}{\partial^2 x} + k_0^2 p = 0 \tag{1}$$

where the wave number k_0 in the fluid medium equals ω/c_0, ω is the angular frequency and c_0 is the speed of sound in the fluid medium.

Fluid load p should satisfy the Sommerfeld boundary condition at the infinity boundary, which can be written as

$$\lim_{R \to \infty} R\left(\frac{\partial p}{\partial R} + ik_0 p\right) = 0 \tag{2}$$

Considering the finite cylindrical shell attached with both infinite rigid baffles, the analytical solution of the sound pressure at a field point (r, θ, x) could be written as

$$p = \sum_{\alpha=0}^{1}\sum_{n=0}^{\infty}\sum_{m=0}^{\infty} P_{mn} H_n^{(1)}(k_r r)\cos(k_m x)\sin\left(n\theta + \frac{\alpha\pi}{2}\right) \tag{3}$$

where $k_m = \dfrac{m\pi}{L}, m = 0,1,...N$, $k_r = \sqrt{k_0^2 - k_m^2}$.

The fluid load p also should satisfy Neumann boundary condition at the fluid-solid coupling interface. The Neumann boundary condition can also be written as

$$-\frac{1}{i\omega\rho}\frac{\partial p}{\partial r} = \frac{\partial w}{\partial t}\Big|_{r=R}, 0 \le x \le L \tag{4}$$

where ρ is the fluid density, w is the radial displacement of cylindrical shell, R is the radius of the cylindrical shell, L is the length of the cylindrical shell.

2.2 Ice model

In the dynamic behavior analysis of the elastic structure, the plastic deformation and failure of ice are neglected when only considering the small deformation. The ice is simplified as a horizontally smooth elastic layer, which floats on the water surface and 10% volume is higher than surface without external load called "freeboard". Normally, ice is divided into the upper layer and lower layer along with the depth of the layer [23]. Ice density is about 90% of the water density. Multi-year ice that has less salt, pores and stronger than one-year ice can be approximately regarded as isotropic. The Arctic sea ice is mostly multi-year ice, so the ideal elastic material is employed to simulate the ice model. The physical and mechanical parameters of ice [24] are shown in Table.1.

2.3 Cylindrical shell

The finite element formulas for the vibration analysis of the cylindrical shell can be written as

$$M\ddot{\delta} + K\delta = F^m + F^p \tag{5}$$

where F^m is structural equivalent nodal load resulted from external excitation, F^p is the fluid equivalent nodal load, δ is displacement response vectors of the cylindrical shell. K and M represent the integral stiffness matrix and mass matrix, respectively, which are obtained by the integration of the stiffness matrix K_e and mass matrix M_e of shell elements.

Both element stiffness matrix K_e and element mass matrix M_e can be written as

$$K_e = \iint_S B_\delta^T D B_\delta ds \, , \quad M_e = \rho_s \iint_S N_\delta^T N_\delta ds \tag{6}$$

where ρ_s is the material density of the cylindrical shell, N_δ is the displacement shape function matrix of the tetrahedral element, D is the elastic matrix of shell elements.

Equivalent node load F^p of sound pressure in fluid acting on the fluid-structure interfaces can be obtained as

$$F^p = \sum_e \iint_{Se} N_\delta^T n_l N_\delta dS \times P \tag{7}$$

Comparing the above formula with the acoustic-structure coupling matrix:

$$F^p = R^T P \tag{8}$$

where R is acoustic-structure coupling matrix, P is sound pressure vector of the whole element nodes on the

fluid-structure interfaces

After substituting Eq. (8) into Eq. (5) and combining with Eq. (4), the governing equation of acoustic-structure coupling system can be written as

$$\begin{bmatrix} -R^T & K^s - \omega^2 M^s \\ K^p - C_\Phi - \omega^2 M^p & -\rho_0 \omega^2 R \end{bmatrix} \begin{Bmatrix} P \\ \delta \end{Bmatrix} = \begin{Bmatrix} F^m \\ C_0 \end{Bmatrix} \tag{9}$$

The displacement vectors of the cylindrical shells and sound pressure in the fluid medium can be numerically calculated directly. The acceleration data are converted into a vibration acceleration level L_a by $20\lg(a/a_0)$, where a is the acceleration value and a_0 is the base acceleration 1e-6 m/s^{-2}. The sound pressure is converted into a sound pressure level L_p by $20\lg(p/p_0)$, where p is the experimental test data and p_0 is the base acceleration 1 μpa.

3 Experimental verification

The cylindrical shell model is designed and made from Q235 steel. The geometrical dimensions and material properties of the cylindrical shell are: Length L=0.7m, thickness t=2mm, radius R=0.15m; section size of the ring-stiffener is 5mm×2mm with its spacing Δl=0.098m. The density of the steel ρ_s equals 7850 kg/m^3, the elastic modulus of the steel E=2.06e11 Pa, the Poisson's ratio μ=0.3 and damping loss factor η=0.01. 15mm thick caps are attached with both ends of the cylindrical shell. fluid density ρ_f equals 1000kg/m^3, sound velocity c_f equals 1500m/s. After welding the lifting lug at the end cover, the test model is elastically suspended in the air by a flexible rope, as shown in Fig. 1(a) and Fig. 1(b). Taking advantage of axisymmetric features of the cylindrical shell, several measuring points are laid up to record the vibration acceleration data along the circumferential and axial direction. 1 force sensor (PCB-208C02) and 7 acceleration sensors (PCB-352C03) are arranged to receive the radial acceleration data. The radial excitation force acts on position 1(0.15, 0°, 0.35) with unit amplitude. Moreover, 3 Hydrophones (B&K-8104) are laid up in the anechoic tanks to obtain sound pressure data. The specific experimental detail including the layout of measuring points is described in Ref. [19].

The natural frequencies of the clamped cylindrical shell for each order (m, n) can be solved by coupled FEM and BEM. The comparison between numerical results and experiment results is illustrated in Table 2. It

can be found that the natural frequencies from the numerical model in vacuo are in coincide with experiment results in air. Considering that the effect of weak acoustic-structure coupling is ignored in numerical calculation, this results in a numerically calculated value that is less than the experimental value. The relative difference is less than 4%, which proves the numerical method is effective and reliable to analyze the free vibration analysis of the cylindrical shell.

The experimental model is also employed to verify the forced vibration and acoustic responses calculated by coupled FEM and BEM. The boundary conditions of the cylindrical shell models are equivalent to be clamped at both ends. The vibration acceleration and sound pressure data at different measuring points were collected to obtain the vibration acceleration level L_v and sound pressure level L_p in the frequency range 5Hz-1500Hz. The dynamic responses of the experimental model of the cylindrical shell subject to the harmonic force excitation are compared with the relevant numerical results from coupled FEM and BEM, as shown in Fig. 2.

In the 5Hz-1500 Hz band, it can be observed that the vibration acceleration level calculated by coupled FEM and BEM coincided very well with experimental results, except some loss of resonance peaks in low frequency. this is due to the natural frequencies of the end cap, which is corresponding to the peak frequency around 14 Hz. The amplitudes of both vibration results are slightly different at the peak frequencies, the resonance peak numbers of experiment model are denser than that of numerical results. No matter frequency peaks and variation trend of sound pressure level curves, the numerical results and experimental results agree well on the whole frequency range except low-frequency range 5Hz-180Hz. The sound pressure results from the experiment test are larger than those of the numerical results. This is due to the local vibration of both thick end caps and seal flange. Overall, the numerical results are coincident with the experimental results. It is effective and reliable for the numerical method to analyze the vibro-acoustic characteristics of the immersed cylindrical shell.

4 Results and discussions

4.1 fully immersed cylindrical shell

The effects of ice thickness and immersion depth on the radial quadratic velocity and acoustic radiation of fully immersed cylindrical shell are investigated in this section. The geometrical dimensions and material

properties of the cylindrical shell are given as: the length L=0.7m, the radius R=0.15m, the thickness t=2mm, the elastic modulus E=206GPa, the Poisson's ratio μ=0.3, the density ρ_s=7850kg/m³, the damping loss factor $\eta = 0.01$. the fluid density ρ_f = 1000kg/m³, the sound velocity c_f=1500m/s. The radial excitation force in the cylindric coordinate system acts on the position ($L/2$, 270°) with unit amplitude. Four-node shell elements are employed to generate quad meshes of the cylindrical shell, the size of which is set to 0.04m. Both ends of the cylindrical shell are assumed to be simply supported boundary conditions. The distance H from the axes of the cylindrical shell to the lower surface of the ice layer is set to 0.3m. The flow field radius is taken as 2m. A hemispherical flow field meshed by AC3D4 acoustic tetrahedral elements, the size of which is from 0.04m to 0.125m. The brick element size of ice model is 0.04m. the distance between the central line and lower surface is 0.3m. The hydrophone (BK-8104) is positioned 1.2 m from the axes of the cylindrical shell to collect the underwater sound pressure, as seen in Fig. 3(b). Generally, a submarine's diameter is about 10 meters. And the thickness of sea ice can reach 3 meters [1~3]. Then, ice thickness is close to D/3. The ratio of ice thickness to the diameter D as a nondimensional parameter is employed to accord with the actual case.

A tie constraint is defined at the interface of the acoustic field and cylindrical shell. A non-reflective impedance boundary condition is defined at the outer surface of the flow field to numerically simulate the infinite fluid domain. Another tie constraint is defined at the interface of the flow field and ice layer. The ice layer is divided into upper and lower ice layers, which are meshed by hexahedral meshes and tetrahedron meshes respectively. Effect of the ice thickness on vibro-acoustic characteristics of the fully immersed cylindrical shell is analyzed, as shown in Fig. 4. Although it has little influence on the structural vibration response in frequency range 5Hz-2000 Hz band, both the sound power level and radiation efficiency decrease slightly with the ice thickness increase in 600Hz-2kHz. As for the sound pressure level, it decreases obviously especially in the peak frequencies owning to sound absorption of the ice model.

The radiated sound power reflects the whole radiated noise ability of the structure, while the sound directivity reflects the directional characteristics of the generated sound field in ice-covered water. The field

points P located at r=1m are employed to describes the near-field sound pressure. The sound directivity at 600Hz and 1800 Hz is calculated, as shown in Fig.5. It shows that the effect of ice thickness on the sound directivity of the cylindrical shell is not obvious at 600 Hz. Two main lobes appeared at 90 degree and 270 degree, which are almost symmetrical. Sound pressure main lobes appear at 135 degree and 315 degree, and six asymmetric side lobes appear at 1800 Hz when ice doesn't exist. Instead, the main lobes appear at 45 degree and 225 degree.

The distance H between the cylindrical shell and the ice model is taken as 0.3m、0.6m、0.9m to analyze the effect of H/D on vibro-acoustic characteristics of fully immersed cylindrical shell, as shown in Fig. 6. The whole vibration response curves are very close in 5Hz-500 Hz. peak frequencies offset to the left as H/D increases in 500Hz-2kHz. There is a marked change in the sound pressure level as H/D increases. The same is true of the rules for the sound power level and radiation efficiency. Fig.7 shows that two almost symmetrical main lobes also appear in 90 degrees and 270 degrees at 600 Hz. In the case H/D=1, the main lobes appear in 45 degrees and 225 degrees, and there are four asymmetric side lobes at 1800 Hz. In the case H/D=2 and H/D=3, the main lobes appear in 90 degree and more side lobes appear. The main lobes direction will change and more side lobes will appear in higher frequencies.

4.2 partially immersed cylindrical shell

When the cylindrical shell floats on water and contacts with the ice model, there is a surface-to-surface contact defined to numerically simulate the contact interaction between the partially immersed cylindrical shell and ice model. The small contact allows a finite sliding and defines the friction coefficients to be 0.02 in the tangential behavior. The geometrical dimensions and material properties of the partially immersed cylindrical shell follow the same configurations of those defined in Section 4.1. Sound pressure observation points are arranged as shown in Fig.8.

The effect of ice thickness on vibro-acoustic characteristics of the partially immersed cylindrical shell is investigated, as shown in Fig.9. The contact interaction of ice and the shell reduces the natural frequencies of

the cylindrical shell and reduce the vibration of the cylindrical shell. The mean quadratic velocity level of the shell decreases obviously as ice thickness increases. The wet surface area decreases as ice thickness increases, which lead to the reduction of radiation impedance and make vibration energy loss goes up. Also, the contact interaction of ice and the shell causes vibration energy transmitted to the near-field ice, which contributes to the radiated noise. The contact interaction leads to the increase of radiated noise in the 1kHz-2kHz. The sound pressure level is similar to the rules of sound power level.

Two main lobes appear in 90 degrees and 270 degrees, but the two main lobes are asymmetrical at 600Hz, as shown in Fig.10. When there is no ice, the main lobes appear in 270 degrees at 1800Hz. Instead, the main lobes appear in 60 degrees and 240 degrees. And more side lobes appear.

Gow et al. [25] used the cantilever beam method to establish the experimental relationship between bending strength, elastic modulus and temperature. The overall trends of flexural strength and elastic modulus were basically increasing with decreasing temperature. The temperature along the thickness of the ice is assumed to be constant. Four temperature cases including -2°C, -10°C, -20°C and -30°C are selected to analyze the influence of temperature on the vibro-acoustic characteristics, as shown in Fig. 11. The elastic modulus will increase as the temperature decrease, which is equivalent to increasing the bending stiffness and radiation impedance of the ice model. This led to an increase in constraint stiffness of the cylindrical shell in the contact area. The vibration response of cylindrical shells at some peaks is restrained. Because of the enhancement of acoustic-solid coupling and sound reflection of the ice model, the sound radiation will increase at some high-frequency range.

The salinity of seawater is about 35‰ while sea ice is generally about 3-7‰. The salinity of ice reduces with the sea ice ages. The brine volume is usually employed to represent the volume of liquid in sea ice. Langleben and Pounder[27] obtained the relationship between elastic modulus E and the brine volume of sea ice through a series of experiments, $E=10-0.0351v_b$ Gpa. The brine volume of sea ice v_b satisfies $S_i(0.532+49.185/|T|)$, where S_i(‰) represents salinity of sea ice, T(°C) represents the temperature of sea ice.

The brine volume was employed to analyze the effects of salinity on the vibro-acoustic characteristics of cylindrical shells. Effect of brine volume on the vibro-acoustic characteristics of the semi-submerged cylindrical shell is shown in Fig.12. Elastic modulus also will decrease as brine volume increase, which means a decrease in the bending stiffness and radiation impedance of ice model. Due to the small variation in bending stiffness, the vibration response has a little change. The effect of brine volume on the vibration of the cylindrical shell can be ignored. But the decrease of radiation impedance will lead to leads to a decrease in the radiated sound capacity of the cylindrical shell and ability to inhibit the peaks. Although the peaks values of sound radiation will increase, it mainly embodies reduction in the sound pressure level at high-frequency range with brine volume increase.

The effect of angle α that described immersion depth on vibro-acoustic characteristics of partially immersed cylindrical shell is investigated, as shown in Fig.13. When the ice thickness d is assumed to be D/3, three immersion angles including 30 degree, 60 degree and 90 degree are chosen to be analyzed, as shown in Fig.14. Ice layer has a significant effect on the vibro-acoustic characteristics of cylindrical shell in different immersion depth. While the area of cylindrical shell contacted with ice and waters changes as the immersion angles vary. There are larger contact areas between the shell with ice and water as the angle decreases, which increase the radiation impedance and reduce the vibration obviously. The phenomenon relating to immersion angles can be seen in sound power level curves and sound pressure level curves.

In contrast, the regularity of the radiation efficiency level is opposite to the above conclusions. The radiation efficiency goes up as the immersion angle decreases. The contact area of the shell with water get larger as the immersion angle decreases, which increase the acoustic-structure coupling ability. It leads to the enhancement of sound radiation efficiency. Fig.14 shows that two main lobes appear in 90 degree and 270 degree respectively, but the two lobes are asymmetrical at 600 Hz. The higher the immersion angle, the bigger the sound pressure value is. At 1800 Hz, the sound directivity exhibits considerable variation, and more side lobes appeared. A special phenomenon is that the main lobes still appear in 90 degree and 270 degree when

immersion angle is 60 degree.

5 Conclusions

In this paper, vibration and sound radiation of immersed cylindrical shell in ice-covered water are studied based on coupled FEM and BEM. By measuring the vibro-acoustic data, a corresponding test model was designed to demonstrate the effectiveness and practicality of the present numerical method. Comparisons of experiment results and numerical results prove the capability of the numerical model to predict the vibration and acoustic response. Both models of fully immersed and partially immersed cylindrical shell were numerically simulated to analyze the forced vibration and sound radiation. The influence of immersion depth, ice thickness density, temperature and brine volume on vibro-acoustic characteristics of the cylindrical shell were also discussed. It can be concluded that: 1) When the cylindrical shell is fully immersed, the ice layer has little effect on the structure vibration, but the sound radiation will decrease with the ice layer thickness increase; 2) In the partially immersed state, the ice thickness has a great influence on the structure vibration. The contact interaction leads to the increase of radiated noise in the 1kHz-2kHz; 3) At low frequencies, it acts as approximately dipole vibration (bell-shaped vibration), and the sound field directivity is "8" shape. At high frequencies, the sound field directivity tends to be complicated with frequency increase. 4) the effect of density, temperature and brine volume mainly reflects in the high-frequency range.

Acknowledgements

References

1. Rothrock DA, Percival DB, Wensnahan M. The decline in arctic sea-ice thickness: Separating the spatial, annual, and interannual variability in a quarter century of submarine data. J Geophys Res-Oceans 2008; 113(C5).
2. Kwok R and Rothrock DA. Decline in Arctic sea ice thickness from submarine and ICESat records: 1958-2008. Geophys Res Lett 2009; 36(15).

3. Sato K and Inoue J. Comparison of Arctic sea ice thickness and snow depth estimates from CFSR with in situ observations. Clim Dynam 2018; 50(1-2): 289-301.

4. Wolf J, Diachok O, Yang T, et al. Very-low-frequency under-ice reflectivity. J Acoust Soc Am 1993; 93: 1329-1334.

5. El Damatty A, Saafan M and Sweedan A. Dynamic characteristics of combined conical-cylindrical shells. Thin Wall Struct 2005; 43: 1380-1397.

6. Ventsel E, Naumenko V, Strelnikova E, et al. Free vibrations of shells of revolution filled with a fluid. Eng Anal Bound Elem 2010; 34: 856-862.

7. Liu C-H and Chen P-T. Numerical analysis of immersed finite cylindrical shells using a coupled BEM/FEM and spatial spectrum approach. Appl Acoust 2009; 70: 256-266.

8. Ettouney MM, Daddazio RP and Abboud NN. The interaction of a submerged axisymmetric shell and three dimensional internal systems. Int J Numer Meth Eng 1994; 37: 2951-2970.

9. Peters H, Kinns R and Kessissoglou N. Effects of internal mass distribution and its isolation on the acoustic characteristics of a submerged hull. J Sound Vib 2014; 333: 1684-1697.

10. Laulagnet B and Guyader J. Sound radiation by finite cylindrical ring stiffened shells. J Sound Vib 1990; 138: 173-191.

11. Caresta M and Kessissoglou NJ. Structural and acoustic responses of a fluid-loaded cylindrical hull with structural discontinuities. Appl Acoust 2009; 70: 954-963.

12. Caresta M and Kessissoglou NJ. Acoustic signature of a submarine hull under harmonic excitation. Appl Acoust 2010; 71: 17-31.

13. Meyer V, Maxit L, Guyader J-L, et al. Prediction of the vibroacoustic behavior of a submerged shell with non-axisymmetric internal substructures by a condensed transfer function method. J Sound Vib 2016; 360: 260-276.

14. Wang X, Chen D, Xiong Y, et al. Experiment and modelling of vibro-acoustic response of a stiffened submerged cylindrical shell with force and acoustic excitation. Results Phys 2018; 11: 315-324.

15. Wang X and Guo W. Dynamic modelling and vibration characteristics analysis of submerged stiffened combined shells. Ocean Eng 2016; 127: 226-235.

16. Qu Y, Chen Y, Long X, et al. Free and forced vibration analysis of uniform and stepped circular cylindrical shells using a domain decomposition method. Appl Acoust 2013; 74: 425-439.

17. Guo W, Li T, Zhu X, et al. Vibration and acoustic radiation of a finite cylindrical shell submerged at finite depth from the free surface. J Sound Vib 2017; 393: 338-352.

18. Pritchard RS. An elastic-plastic constitutive law for sea ice. Int J Appl Mech 1975; 42: 379-384.

19. Hibler III W. A dynamic thermodynamic sea ice model. J Phys Oceanogr 1979; 9: 815-846.

20. Gagnon R. A numerical model of ice crushing using a foam analogue. Clod Reg Sci Technol 2011; 65: 335-350.

21. Hendrikse H and Metrikine A. Ice-induced vibrations and ice buckling. Clod Reg Sci Technol 2016; 131: 129-141.

22. Mattsson K, Dunham EM and Werpers J. Simulation of acoustic and flexural-gravity waves in ice-covered oceans. J Comput Phys 2018; 373: 230-252.

23. Kaminski T, Kauker F, Toudal Pedersen L, et al. Arctic Mission Benefit Analysis: impact of sea ice thickness, freeboard, and snow depth products on sea ice forecast performance. Cryosphere 2018; 12(8): 2569-2594.

24. Langleben M and Pounder ER. Elastic parameters of sea ice.Ice and Snow,MIT Press 1963; USA: 69-78.

25. Gow AJ and Ueda HT. Structure and temperature dependence of the flexural properties of laboratory freshwater ice sheets. Clod Reg Sci Technol 1989; 16(3): 249-270.

Table Captions

Table 1. Ice physical and mechanical parameters
Table 2. Comparison of the natural frequencies (unit： Hz)
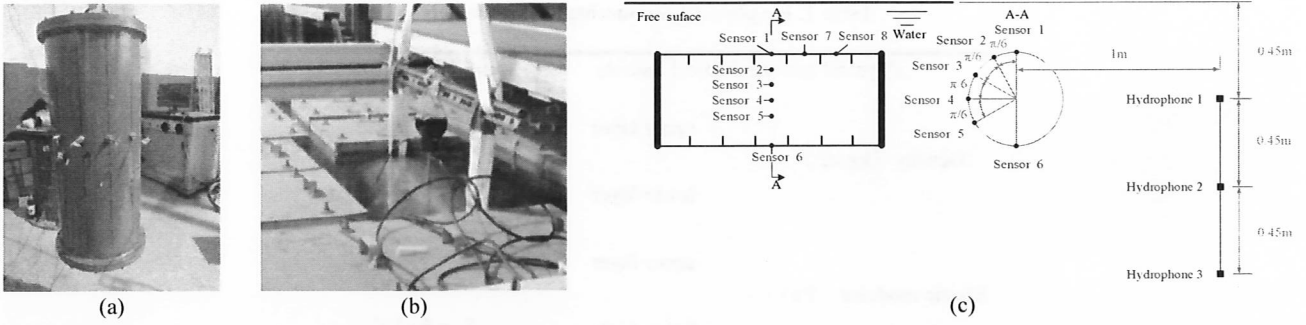
Figure Captions

Fig.1 Experimental setup for the submerged cylindrical shell. Modal test in air (a), vibro-acoustic response test in water (b), and the layout of measuring points in water (c).
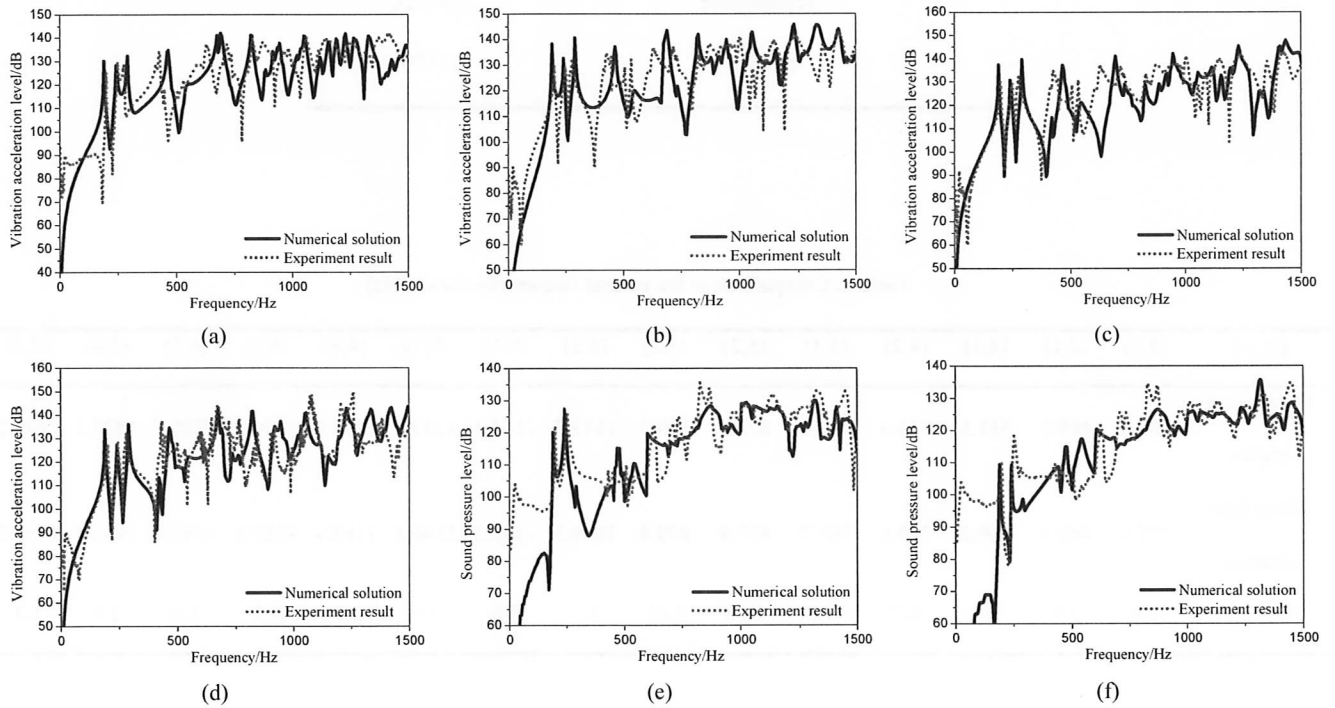
Fig.2 Comparison curves of experimental results and numerical results. Position 2 (a), position 6 (b), position 7(c), position 8 (d), hydrophone 1 (e), hydrophone 2 (f).
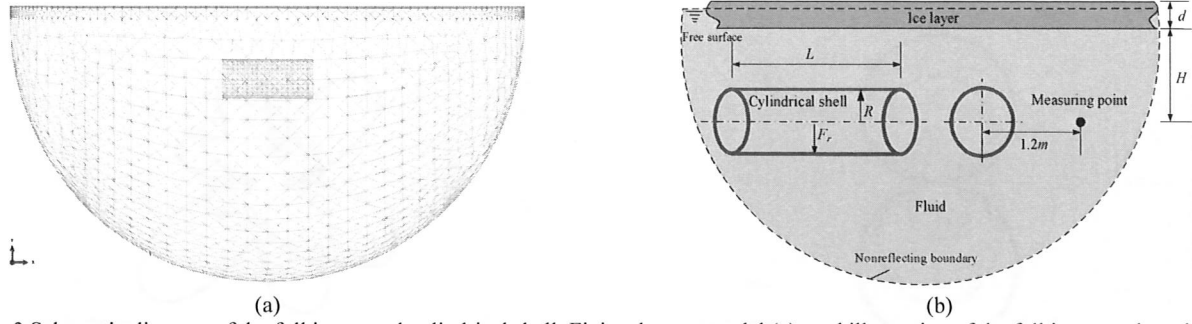
Fig.3 Schematic diagram of the full immersed cylindrical shell. Finite element model (a), and illustration of the full immersed model (b).
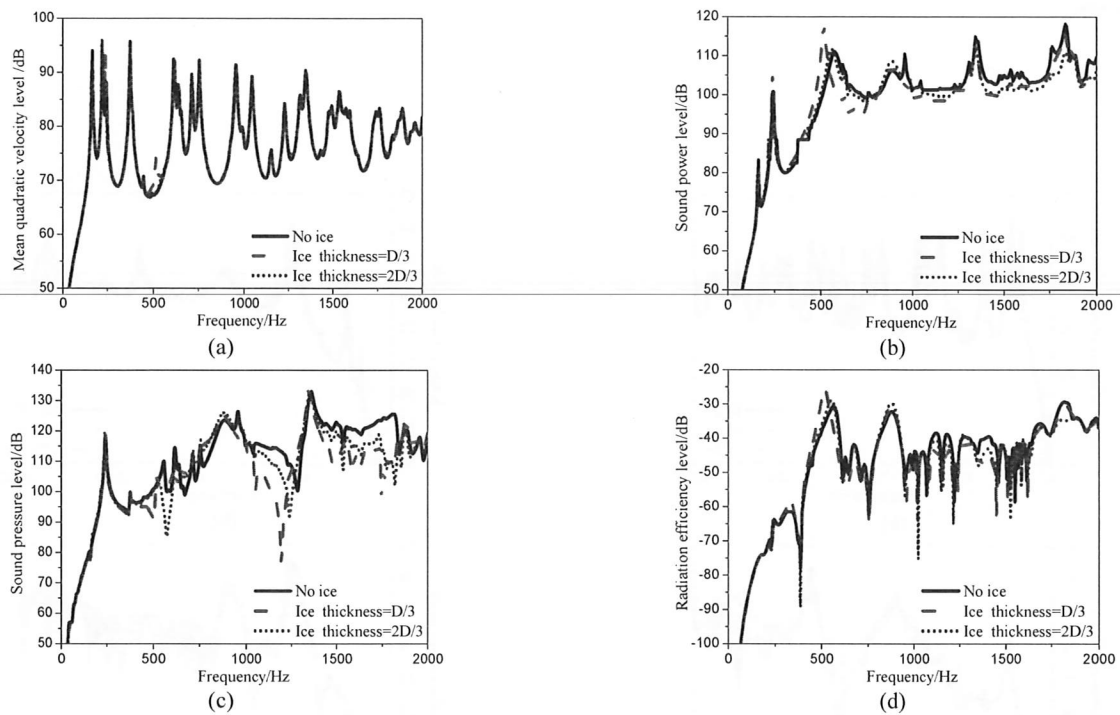
Fig.4 Effect of ice thickness on the vibro-acoustic characteristics of full immersion cylindrical shell. Mean quadratic velocity level (a), sound power level(b), sound pressure level(c), and radiation efficiency level (d).
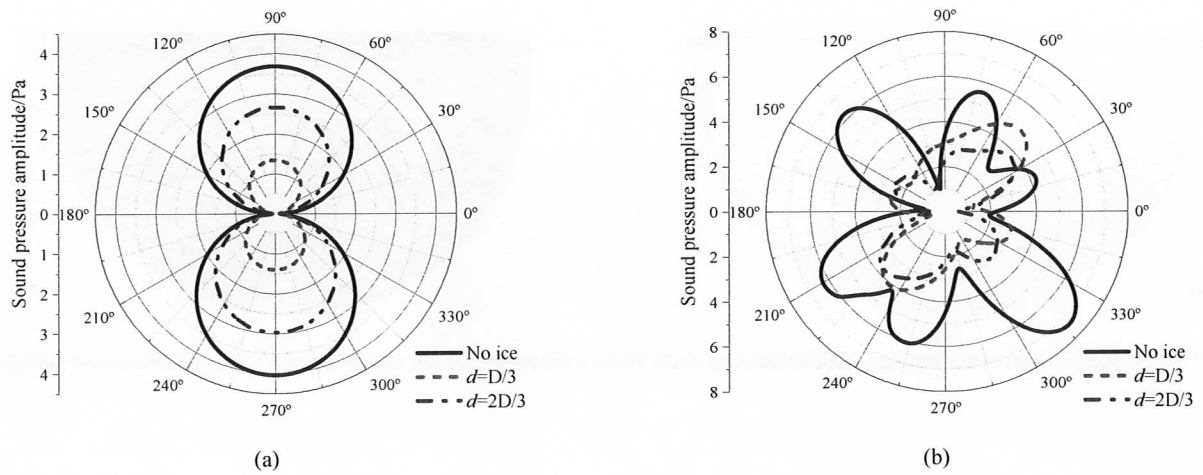
Fig.5 Effect of ice thickness on the sound directivity of full immersion cylindrical shell. Sound directivity at 600 Hz (a), and sound directivity at 1800 Hz (b).
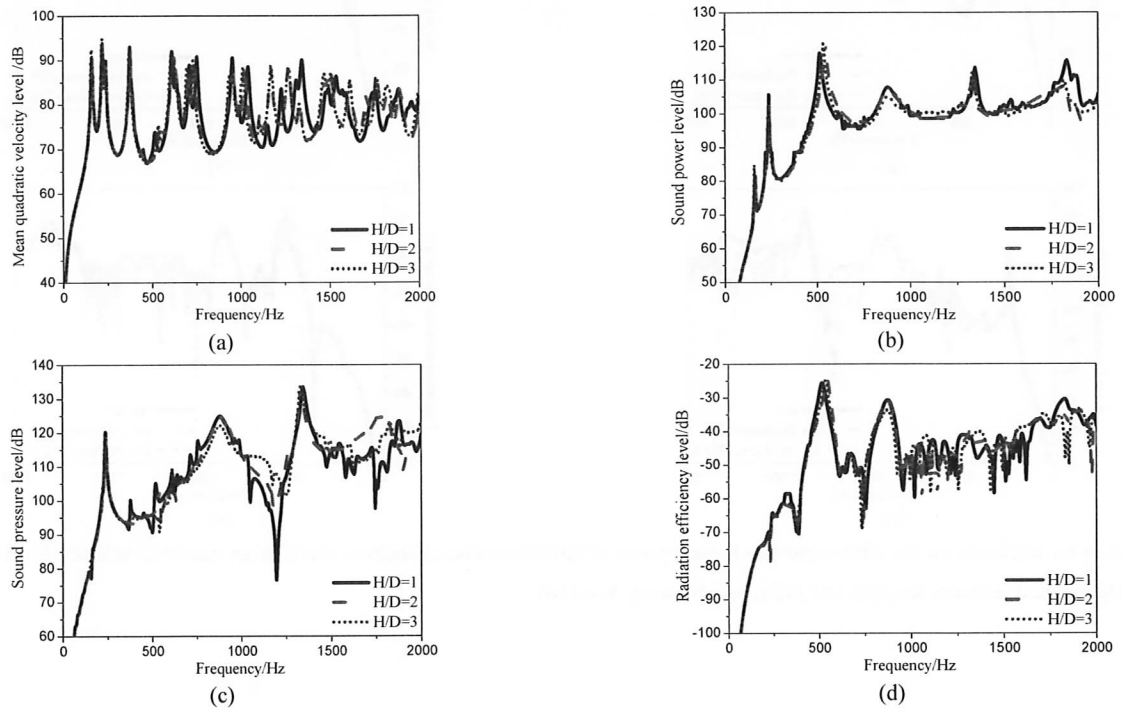
Fig.6 Effect of H/D on the vibro-acoustic characteristics of full immersion cylindrical shell. Mean quadratic velocity level (a), sound power level(b), sound pressure level(c), and radiation efficiency level (d).
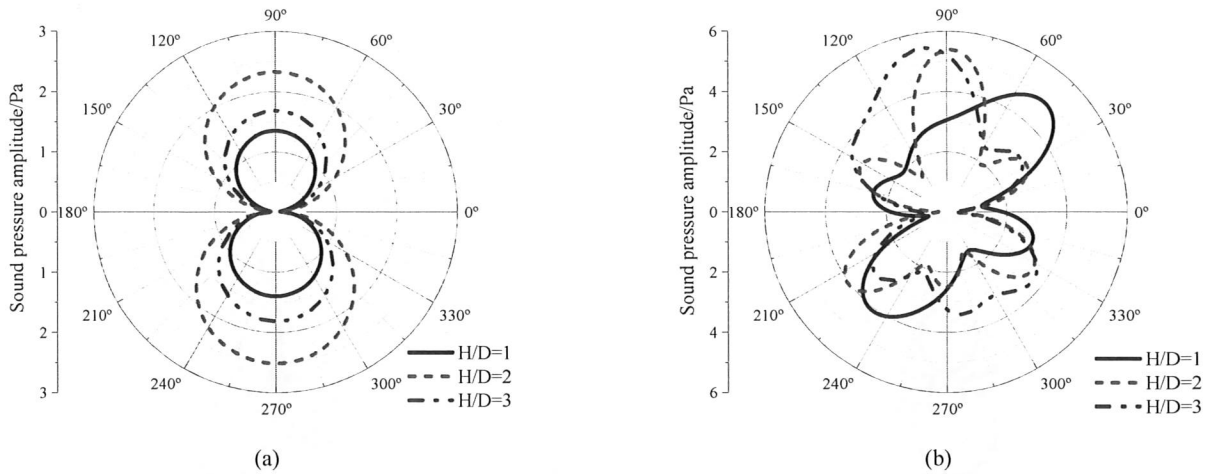
Fig.7 Influence of H/D on the sound directivity of full immersion cylindrical shell. Sound directivity at 600 Hz (a), and sound directivity at 1800 Hz (b).

Fig.8 Schematic diagram of semi-submersible model. Finite element model (a), and illustration of partially immersed model (b).

Fig.9 Influence of ice thickness on the vibro-acoustic characteristics of semi-submerged cylindrical shell. Mean quadratic velocity level (a), sound power level(b), sound pressure level(c), and radiation efficiency level (d).

Fig.10 Effect of ice thickness on the sound directivity of Semi-submerged cylindrical shell. Sound directivity at 600 Hz (a), and sound directivity at 1800 Hz (b).

Fig. 11 effect of temperature on the vibro-acoustic characteristics of the semi-submerged cylindrical shell. Mean quadratic velocity level (a), sound power level(b), sound pressure level(c), and radiation efficiency level (d).

Fig.12 Effect of brine volume on the vibro-acoustic characteristics of the semi-submerged cylindrical shell. Mean quadratic velocity level (a), sound power level(b), sound pressure level(c), and radiation efficiency level (d).

Fig.13 effect of angle α on the vibro-acoustic characteristics of the partial immersed cylindrical shell. Mean quadratic velocity level (a), sound power level(b), sound pressure level(c), and radiation efficiency level (d).

Fig.14 Influence of angle α on the sound directivity of partial immersed cylindrical shell. Sound directivity at 600 Hz (a), and sound directivity at 1800 Hz (b).
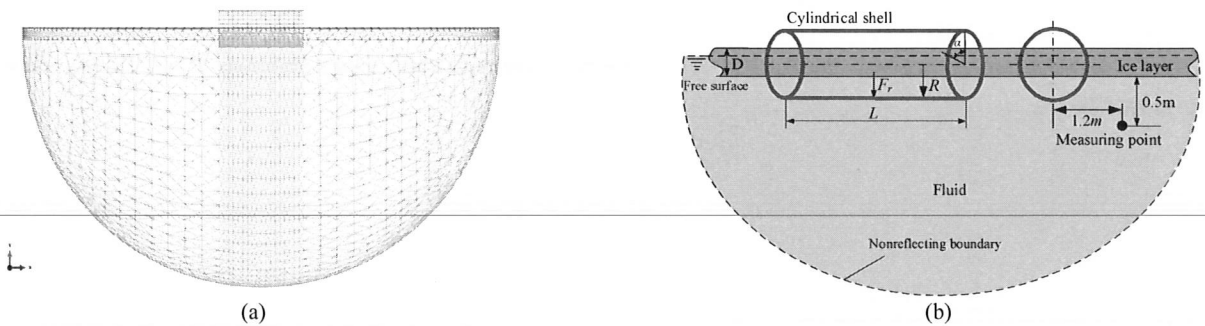
Table 1. Ice physical and mechanical parameters

Physical and mechanical indexes		Material parameters
Density （kg/m³）	upper layer	$\rho_1 = 0.880$
	lower layer	$\rho_2 = 0.910$
Elastic modulus （Pa）	upper layer	$E_1 = 4 \times 10^9$
	lower layer	$E_2 = 6 \times 10^9$
Poisson's ratio		$\sigma = 0.33$
Damping		$\beta = 0.25$
Temperature		$T = -2°C$
Salinity		$\eta = 5‰$

Table 2. Comparison of the natural frequencies (unit：Hz)

(m, n)	(3,1)	(2,1)	(4,1)	(4,2)	(5,1)	(5,2)	(3,2)	(5,3)	(6,1)	(0,1)	(4,3)	(6,2)	(6,3)	(5,4)	(2,2)
Experiment results	357.0	469.3	512.5	735.9	792.9	878.6	879.5	1113.5	1144.1	1153.1	1187.9	1190.2	1320.7	1427.2	1487.0
Numerical solution	355.6	485.9	509.2	730.8	787.7	877.9	879.4	1099.3	1132.2	1140.8	1168.4	1181.2	1302.7	1456.7	1468.2
Error (%)	0.4	3.5	0.6	0.7	0.66	0.08	0.01	1.3	1.0	1.0	1.6	0.8	1.4	2.0	1.2

(a)   (b)   (c)

Fig.1 Experimental setup for the submerged cylindrical shell. Modal test in air (a), vibro-acoustic response test in water (b), and the layout of measuring points in water (c).

(a)   (b)   (c)

(d)   (e)   (f)

Fig.2 Comparison curves of experimental results and numerical results. Position 2 (a), position 6 (b), position 7(c), position 8 (d), hydrophone 1 (e), hydrophone 2 (f).

(a)　　　　　　　　　　　　　　　　　(b)

Fig.3 Schematic diagram of the full immersed cylindrical shell. Finite element model (a), and illustration of the full immersed model (b).
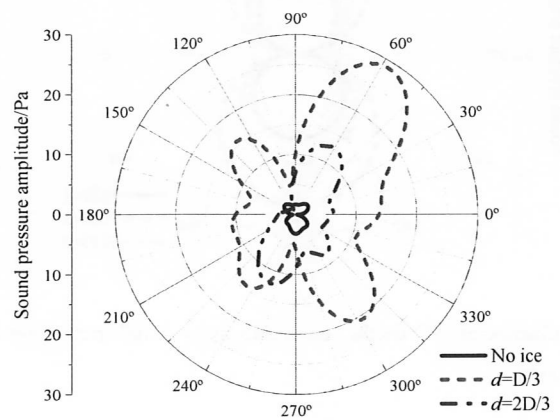

(a)

(b)

(c)

(d)

Fig.4 Effect of ice thickness on the vibro-acoustic characteristics of full immersion cylindrical shell. Mean quadratic velocity level (a), sound power level(b), sound pressure level(c), and radiation efficiency level (d).
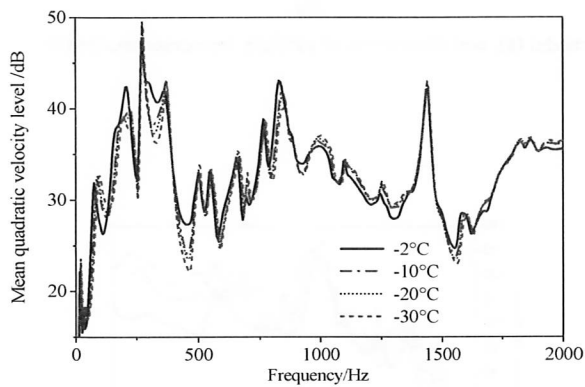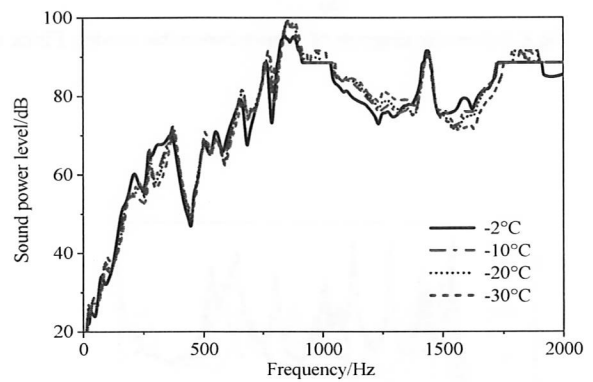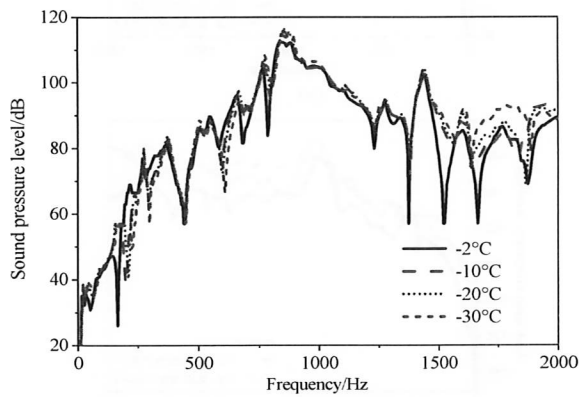
(a)

(b)

Fig.5 Effect of ice thickness on the sound directivity of full immersion cylindrical shell. Sound directivity at 600 Hz (a), and sound directivity at 1800 Hz (b).
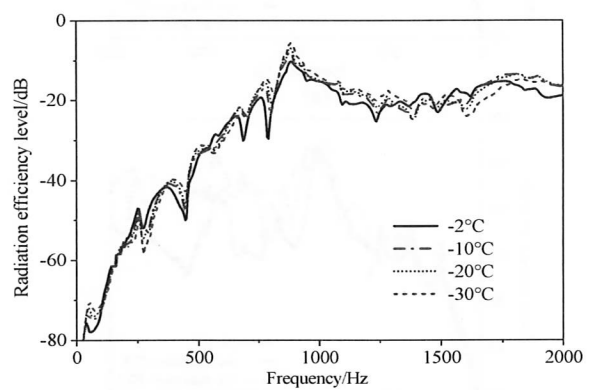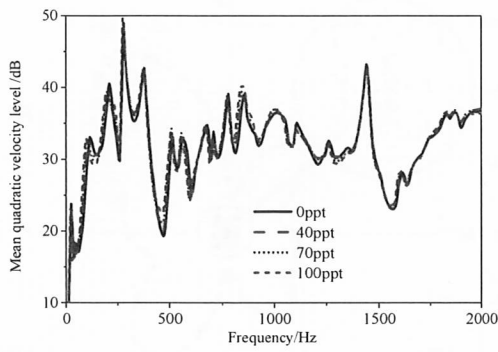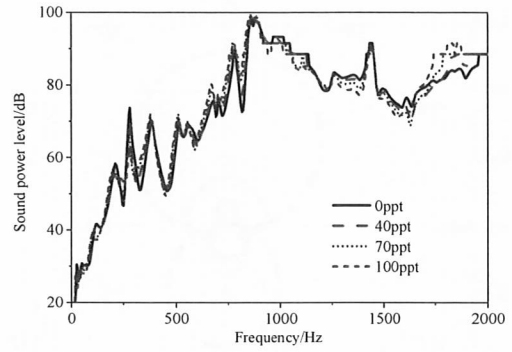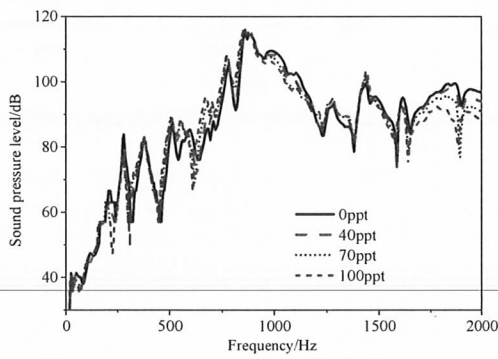

(a)

(b)

(c)

(d)

Fig.6 Effect of H/D on the vibro-acoustic characteristics of full immersion cylindrical shell. Mean quadratic velocity level (a), sound power level(b), sound pressure level(c), and radiation efficiency level (d).

(a)   (b)

Fig.7 Influence of H/D on the sound directivity of full immersion cylindrical shell. Sound directivity at 600 Hz (a), and sound directivity at 1800 Hz (b).

(a)   (b)

Fig.8 Schematic diagram of semi-submersible model. Finite element model (a), and illustration of partially immersed model (b).

(a)   (b)

(c)   (d)

Fig.9 Influence of ice thickness on the vibro-acoustic characteristics of semi-submerged cylindrical shell. Mean quadratic velocity level (a), sound power level(b), sound pressure level(c), and radiation efficiency level (d).

(a)   (b)

Fig.10 Effect of ice thickness on the sound directivity of Semi-submerged cylindrical shell. Sound directivity at 600 Hz (a), and sound directivity at 1800 Hz (b).

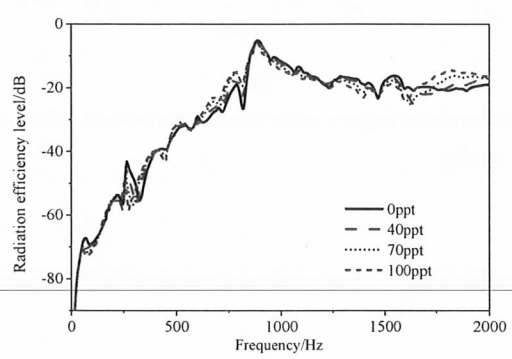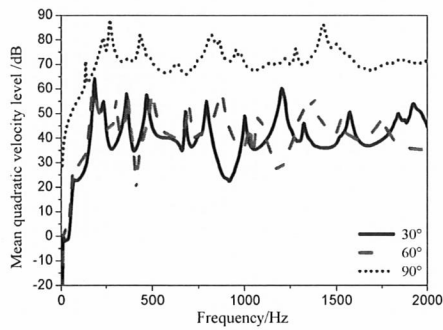(a)   (b)

(c)   (d)

Fig. 11 effect of temperature on the vibro-acoustic characteristics of the semi-submerged cylindrical shell. Mean quadratic velocity level (a), sound power level(b), sound pressure level(c), and radiation efficiency level (d).
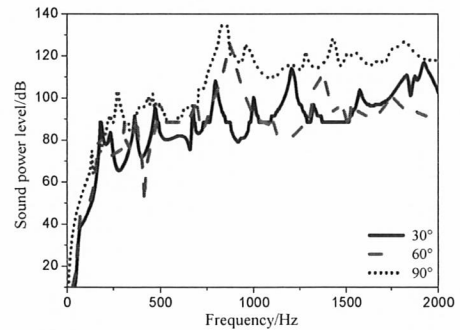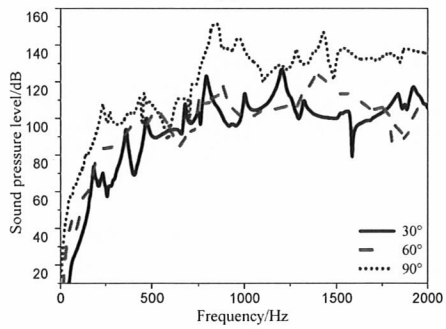
(a)

(b)

(c)

(d)

Fig.12 Effect of brine volume on the vibro-acoustic characteristics of the semi-submerged cylindrical shell. Mean quadratic velocity level (a), sound power level(b), sound pressure level(c), and radiation efficiency level (d).
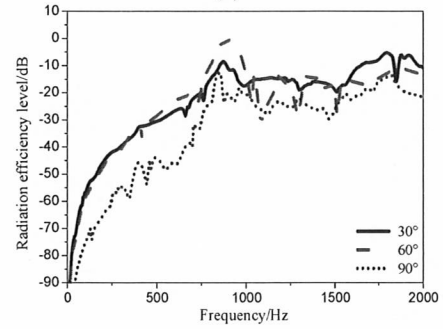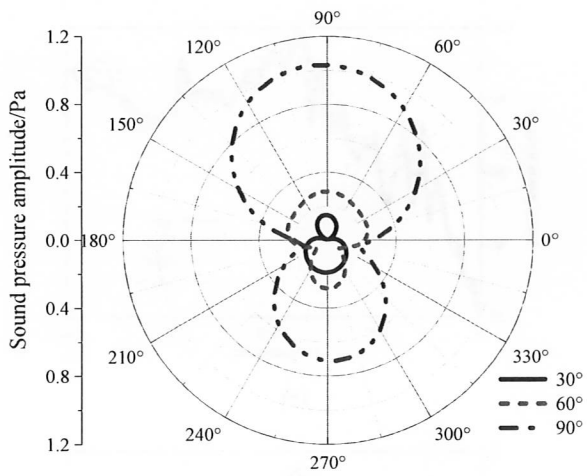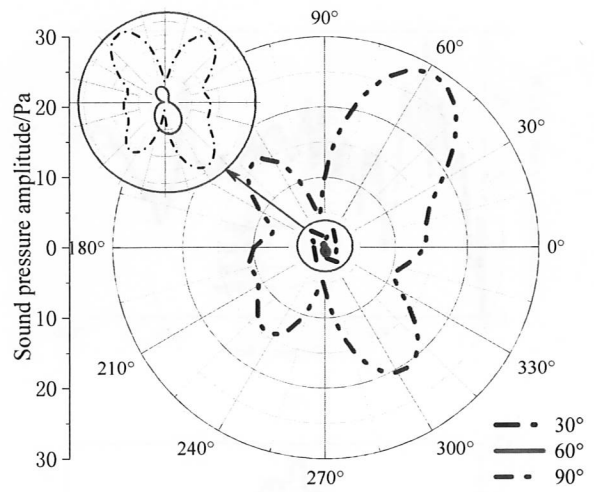

(a)

(b)

(c)

(d)

Fig.13 effect of angle α on the vibro-acoustic characteristics of the partial immersed cylindrical shell. Mean quadratic velocity level (a), sound power level(b), sound pressure level(c), and radiation efficiency level (d).

Fig.14 Influence of angle α on the sound directivity of partial immersed cylindrical shell. Sound directivity at 600 Hz (a), and sound directivity at 1800 Hz (b).

Conflict of interest statement

We declare that we have no financial and personal relationships with other people or organizations that can inappropriately influence our work, there is no professional or other personal interest of any nature or kind in any product, service and/or company that could be construed as influencing the position presented in, or the review of, the manuscript entitled, "Simulation and investigations on the vibro-acoustic behavior of cylindrical shells in ice-covered water".

Dear Editor,

We submit our revised titled "Simulation and investigations on the vibro-acoustic responses of immersed cylindrical shells in ice-covered water" to Results in Physics. This paper has been revised. Neither the entire paper nor any part of its content has been published or has been accepted elsewhere. It is not being submitted to any other journal.

All authors have seen the manuscript and approved to submit to your journal.

Sincerely yours,

X.Z.Wang

Oct. 2th, 2019